Human Molecular Genetics, 2006, Vol. 15, No. 6 ***831–838***
doi:10.1093/hmg/ddl002
Advance Access published on January 30, 2006

A role for *Brca1* in chromosome end maintenance

J. Peter McPherson[1,2,†,‡], M. Prakash Hande[3,4,*,†], Anuradha Poonepalli[3], Benedicte Lemmers[1,2], Elzbieta Zablocki[1,2], Eva Migon[1,2], Amro Shehabeldin[1,2], Annaliza Porras[1,2], Jana Karaskova[2], Bisera Vukovic[2], Jeremy Squire[2] and Razqallah Hakem[1,2]

[1]Advanced Medical Discovery Institute and [2]Ontario Cancer Institute, Department of Medical Biophysics, University of Toronto, Toronto, Ontario, Canada M5G 2C1, [3]Department of Physiology, Yong Loo Lin School of Medicine, National University of Singapore, Singapore 117597, Singapore and [4]Oncology Research Institute, National University Medical Institutes, Singapore 117597, Singapore

Received December 7, 2005; Revised and Accepted January 21, 2006

The role of *BRCA1* in breast and ovarian tumor suppression has been primarily ascribed to the maintenance of genome integrity. BRCA1 interacts with components of the non-homologous end-joining pathway previously shown to play a role in telomere maintenance in yeast. Here, we provide evidence that links Brca1 with telomere integrity. *Brca1*$^{-/-}$ T-cells display telomere dysfunction in both loss of telomere repeats as well as defective telomere capping. Loss of Brca1 synergizes with p53 deficiency in the onset and frequency of tumorigenesis. Karyotyping of *tBrca1*$^{-/-}$ *p53*$^{-/-}$ thymic lymphomas revealed the presence of telomere dysfunction accompanied by clonal chromosomal translocations. The telomere dysfunction phenotype in Brca1-deficient cells suggests that loss of telomere integrity might contribute to chromosome end dysfunction and permit the formation of potentially oncogenic translocations.

INTRODUCTION

Mutations in the breast cancer susceptibility gene *BRCA1* confer genetic predisposition to early-onset familial breast and ovarian cancer (1). Although the BRCA1 protein has been shown to impact the maintenance of genome integrity, transcriptional regulation and chromatin remodeling, the exact mechanism responsible for the tumor suppressor function of BRCA1 remains unknown (1,2). *BRCA1*-associated mammary gland tumors in humans and murine cells deficient in *Brca1* exhibit genomic imbalances and chromosomal aberrations that are hallmarks of genomic instability (1,3,4). As elevated frequencies of chromosomal aberrations are correlated with an increased risk for cancer, the tumor suppressor function of BRCA1 has been linked to its role in genome surveillance. However, dissection of the role of BRCA1 in maintaining genome integrity has been complicated by studies that link BRCA1 to multiple DNA repair pathways, such as homologous-recombinational repair (5), non-homologous end joining (6) and nucleotide excision repair (7).

The study of BRCA1 function *in vivo* is complicated by its essential role in cellular viability, in that disruption of *Brca1* in the absence of additional compensatory mutations results in lethality (3,8–11). Mice that are *tBrca1*$^{-/-}$ carry a targeted null mutation of *Brca1* restricted to the T-cell compartment, resulting in a drastic depletion of thymocytes and peripheral T-cells, the accumulation of chromosomal abnormalities and activation of p53 (12). Thymocyte development in *tBrca1*$^{-/-}$ mice is restored in the absence of p53 or the presence of overexpressed Bcl2. As perturbations in telomere length and/or structure have been identified as mechanisms that contribute to genomic instability (13–15), *tBrca1*$^{-/-}$ cells in the absence of p53 or the presence of overexpressed Bcl2 were analyzed for chromosomal telomere integrity and the presence of telomere-associated chromosomal damage.

RESULTS

Proliferation and developmental defects of *Brca1*$^{-/-}$ T-cells complicate the analysis of mature T-cells (12). Accordingly, *ex vivo* analysis of *Brca1*$^{-/-}$ T-cells was performed in *bcl2* transgenic or *p53* nullizygous backgrounds which rescue thymic development. In order to assess whether Brca1

*To whom correspondence should be addressed at: Department of Physiology, Yong Loo Lin School of Medicine, National University of Singapore, Block MD9, 2 Medical Drive, Singapore 117597, Singapore. Tel: +65 65163664; Fax: +65 67788161; Email: phsmph@nus.edu.sg
†The authors wish it to be known that, in their opinion, the first two authors should be regarded as joint First Authors.
‡Present Address: Department of Pharmacology, University of Toronto, Toronto, Ontario, Canada M5S 1A8.

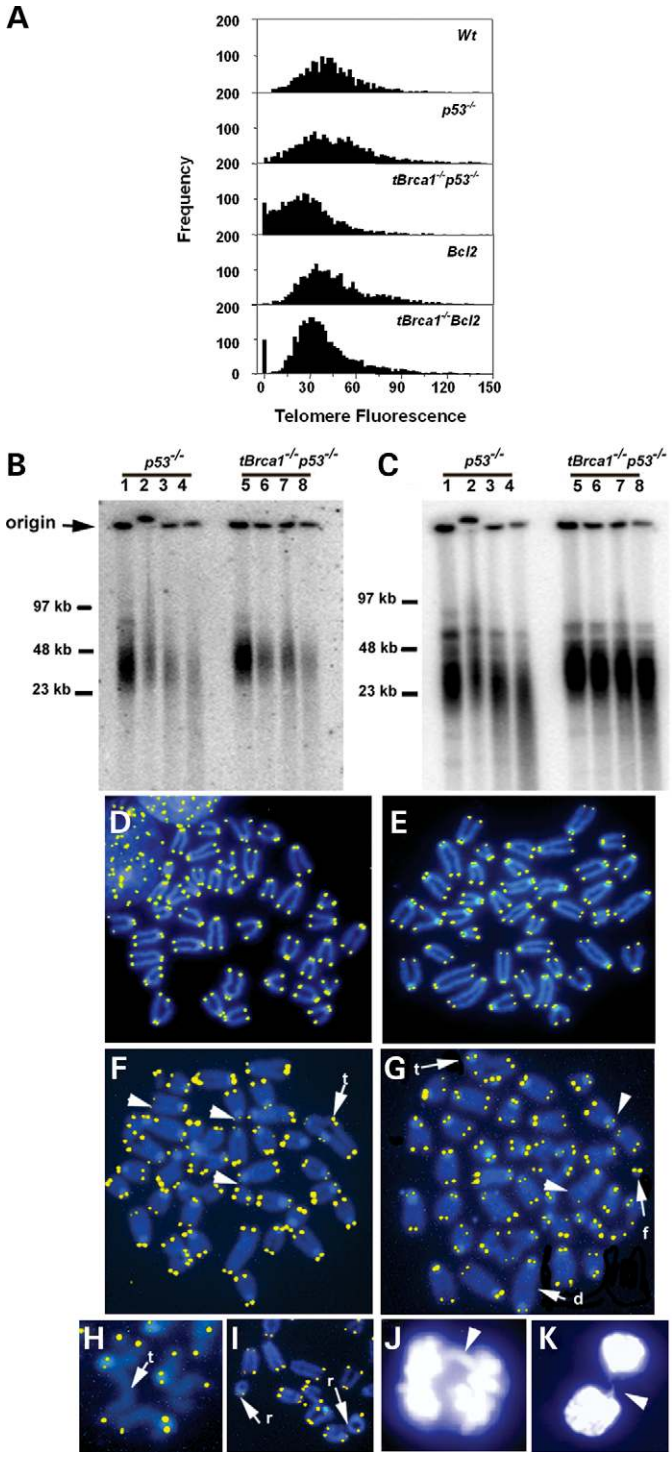

Figure 1. Telomere erosion and chromosomal abnormalities in Brca1-deficient peripheral activated T-cells. (**A**) Representative frequency distributions of telomere fluorescence data collected from qFISH analysis of metaphase chromosomal spreads of $tBrca1^{-/-}p53^{-/-}$ compared with $p53^{-/-}$ and $tBrca1^{-/-}bcl2$ compared with *bcl2* activated T-cells. The *x*-axis depicts the intensity of each signal as expressed in telomere fluorescence units (TFU; 1 TFU = 1 kb of telomeric repeats), the *y*-axis shows the frequency of telomeres of a given length. (**B**) Non-denaturing in-gel hybridization of genomic DNA from $p53^{-/-}$ (lanes 1–4) and $tBrca1^{-/-}p53^{-/-}$ (lanes 5–8) activated T-cells with radiolabeled $(CCCTAA)_4$ oligonucleotide. Specificity of signal was ensured by the stepwise reduction in intensity following incubation with increased amounts of Mung bean nuclease (0 units, lanes 1 and 5; 10 units, lanes 2 and 6; 40 units, lanes 3 and 7; 160 units, lanes 4 and 8). (**C**) To control for non-specific degradation in (B), the same gel is shown following denaturation and subsequent hybridization with radiolabeled $(CCCTAA)_4$. Results shown in (B) and (C) are representative of four independent experiments using T-cells from $p53^{-/-}$ and $tBrca1^{-/-}p53^{-/-}$ siblings derived from three different litters. (**D**–**I**) Telomere-FISH analysis of metaphase chromosomal spreads from $p53^{-/-}$ (D) *bcl2* (E) $tBrca1^{-/-}p53^{-/-}$ (F and I) and $tBrca1^{-/-}bcl2$ (G and H) activated T-cells. Arrowheads denote chromosome ends with reduced telomere signal, t-triradial-like, d-dicentric, f-fragment, r-ring chromosome. (**J** and **K**) Representative anaphase chromosome bridge (J, arrowhead) and chromatin bridge (K, arrowhead) from newly divided daughter $tBrca1^{-/-}p53^{-/-}$ cells. Results shown in (J) and (K) are representative of three independent experiments using T-cells from $p53^{-/-}$ and $tBrca1^{-/-}p53^{-/-}$ siblings derived from three different litters. Telomere fluorescence intensity in pictures shown in (D–I) are for qualitative display only and is not meant to be quantitative in nature.

disruption impacts telomere integrity, the length of telomeric TTAGGG repeats in activated peripheral T-cells from $tBrca1^{-/-}p53^{-/-}$ mice and $p53^{-/-}$ mice were measured using quantitative fluorescence *in situ* hybridization (qFISH) (16). This methodology facilitates the quantitation of telomere repeat sequences from individual chromosome ends and the subsequent analysis of telomeric length distribution, as murine telomeres have large inter-chromosomal variations in the number of TTAGGG repeats. Analysis was conducted on metaphase chromosome spreads prepared using activated peripheral T-cells from sibling cohorts consisting of one $tBrca1^{-/-}p53^{-/-}$ mouse and one $p53^{-/-}$ mouse, for a total of three different cohorts (Fig. 1A and Table 1). In all three cohorts, the average length of telomeres from the $tBrca1^{-/-}p53^{-/-}$ peripheral T-cells was reduced when compared with the $p53^{-/-}$ controls. T-cells from $p53^{-/-}$ mice have equivalent telomere lengths when compared with cells from wild-type mice (Fig. 1A). The absence of p53 was not required for the observed reduction in telomere length in $tBrca1^{-/-}$ T-cells, as loss of telomere repeats was also observed in $tBrca1^{-/-}$ cells in a transgenic *bcl2* background when compared with controls (Fig. 1A and Table 1). Unlike $tBrca1^{-/-}p53^{-/-}$ peripheral T-cells, $tBrca1^{-/-}$ *bcl2* T-cells exhibit a profound proliferation block in response to activation. $tBrca1^{-/-}$ *bcl2* T-cells displayed a less dramatic yet reproducible decrease in average telomere length when compared with *bcl2* T-cell controls. The greater reduction in telomeric sequence in the concomitant absence of p53 might reflect the more efficient elimination of cells with shorter telomeres in the presence of a p53-dependent damage response (17). Similar studies performed on these cells using flow-FISH were consistent with data obtained using qFISH (data not shown). Taken together, these findings indicate a role for Brca1 in maintenance of telomere length.

Telomerase activity was observed in $tBrca1^{-/-}p53^{-/-}$ and $p53^{-/-}$ cells (data not shown), suggesting that telomere erosion was not due to a lack of telomerase activity. There were no obvious alterations in the subcellular localization of TRF1 and TRF2 to punctate nuclear foci (18,19) by indirect immunofluorescence of $tBrca1^{-/-}p53^{-/-}$ cells compared to $p53^{-/-}$ cells (data not shown). Telomere termini end in G-rich single-stranded 3′-overhangs that are required for proper telomere structure and protect against chromosomal

Table 1. Telomere shortening in *tBrca1*$^{-/-}$ peripheral T-cells

	Genotype[a]	Telomere Fluorescence[b] p-arm	q-arm	All telomeres (mean ± SE)
Cohort 1[c]	*L*$^{+/-}$*p53*$^{-/-}$	37.0 ± 0.6	56.3 ± 0.8	46.7 ± 0.5
	cLLp53$^{-/-}$	22.4 ± 0.5	34.3 ± 0.6	28.3 ± 0.4[d]
Cohort 2	*LLp53*$^{-/-}$	36.6 ± 0.4	45.3 ± 0.5	41.0 ± 0.3
	cLLp53$^{-/-}$	33.8 ± 0.4	39.8 ± 0.5	36.9 ± 0.3[d]
Cohort 3	*cL*$^{+/-}$*p53*$^{-/-}$	38.1 ± 0.5	44.6 ± 0.6	41.2 ± 0.4
	cLLp53$^{-/-}$	32.2 ± 0.3	39.4 ± 0.4	35.8 ± 0.3[d]
Mean	*p53*$^{-/-}$			42.9 ± 0.3
	tBrca1$^{-/-}$*p53*$^{-/-}$			33.8 ± 0.2
Cohort 1[c]	*cL*$^{+/-}$*Bcl2*	44.5 ± 0.5	56.9 ± 0.8	50.6 ± 0.5
	cLLBcl2	39.1 ± 0.5	38.4 ± 0.5	38.8 ± 0.4[d]
Cohort 2	*LLBcl2*	41.6 ± 0.6	51.7 ± 0.7	46.6 ± 0.5
	cLLBcl2	33.2 ± 0.4	44.4 ± 0.7	38.9 ± 0.4[d]
Cohort 3	*LLBcl2*	35.6 ± 0.5	39.1 ± 0.6	37.3 ± 0.4
	cLLBcl2	32.3 ± 0.4	37.8 ± 0.4	35.1 ± 0.3[d]
Mean	*Bcl2*			45.2 ± 0.3
	tBrca1$^{-/-}$*Bcl2*			37.6 ± 0.2

Wild-type data for telomere fluorescence (TFU, mean ± SE): p-arm: 39.1 ± 0.6; q-arm: 48.1 ± 0.8; all telomeres: 43.5 ± 0.5. A minimum of 1800 individual telomeres per sample was analyzed (6418 telomeres for p53$^{-/-}$ mice, 7472 telomeres for *tBrca1*$^{-/-}$ *p53*$^{-/-}$ mice, 6578 telomeres for *Bcl2* mice and 8050 telomeres for *tBrca1*$^{-/-}$*Bcl2* mice).

[a]*c*, mouse contains one allele of the *Lck-cre* transgene; *L*$^{+/-}$, mouse is heterozygous for the Brca1 conditionally disrupted allele; *LL*, mouse is homozygous for the Brca1 conditionally disrupted allele. *tBrca1*$^{-/-}$ mice are genotyped as *cLL*.

[b]Telomere fluorescence intensity expressed as TFU, where 1 TFU corresponds to 1 kb of $(T_2AG_3)_n$ sequence.

[c]Each cohort represents two sibling mice of the indicated genotypes. All cohorts are derived from independent litters produced by heterozygous parents, one of which carries the *cre* transgene.

[d]Statistically significant $P \leq 0.001$ in a Mann–Whitney rank sum test; statistical analysis was performed at individual telomere level.

end-to-end fusions (19,20). The integrity of telomeric 3′-overhangs was assayed in genomic DNA from *tBrca1*$^{-/-}$*p53*$^{-/-}$ and *p53*$^{-/-}$ activated T-cells using non-denaturing in-gel hybridization (20). Single-stranded 3′-overhangs were detected in genomic DNA from both *tBrca1*$^{-/-}$*p53*$^{-/-}$ and *p53*$^{-/-}$ cells, as demonstrated by the stepwise reduction of signal following incubation with increasing amounts of the single-strand-specific Mung Bean nuclease (Fig. 1B). To ensure the integrity of double-stranded genomic DNA following nuclease treatment, the same probe recognized telomere restriction fragments following denaturation of the same gel and subsequent hybridization (Fig. 1C). Quantitative analyses from four independent experimental sets did not reveal any significant difference in the integrity of single-stranded 3′-overhangs from *tBrca1*$^{-/-}$*p53*$^{-/-}$ and *p53*$^{-/-}$ activated T-cells (representative experiments depicted in Fig. 1B–C).

Metaphases from *tBrca1*$^{-/-}$ *bcl2* and *tBrca1*$^{-/-}$*p53*$^{-/-}$ activated T-cells show a marked increased incidence of end-to-end fusions (ring chromosomes, dicentric chromosomes and Robertsonian fusions) when compared with *bcl2* and *p53*$^{-/-}$ T-cells, respectively (Fig. 1D–I and Table 2). Of note, end-to-end fusions with detectable telomere signal at the fusion point are markedly increased (Table 2), suggestive of defective telomere capping (13). Mammalian cells with dysfunctional telomeres display increased frequency of anaphase chromosome bridges (19,21). Interestingly, the frequency of anaphase bridges per mitotic events was found to be elevated in *tBrca1*$^{-/-}$*p53*$^{-/-}$ cells (50.7 ± 1.8%) when compared with *p53*$^{-/-}$ cells (13.3 ± 2.3%) (Fig. 1J–K). The increased accumulation of chromosomal fragments detected in *tBrca1*$^{-/-}$*bcl2* and *tBrca1*$^{-/-}$*p53*$^{-/-}$ cells (Table 2) could be the result of catastrophic mitotic shearing in cells with fused chromosomes (19,22).

In the thymus, *Brca1* and *p53* mutations were found to potentiate the formation of thymic lymphomas (23). All *tBrca1*$^{-/-}$*p53*$^{-/-}$ mice develop CD4$^+$CD8$^+$ thymic lymphomas (Fig. 2A) and are moribund or die at a decreased latency (91 ± 41 days, mean age ± SD, $n = 20$) when compared with *tBrca1*$^{+/-}$*p53*$^{-/-}$ mice (179 ± 80 days, $n = 20$) and *p53*$^{-/-}$ mice (155 ± 90 days, $n = 15$), which develop thymic lymphomas or other tumors. A small subset of *tBrca1*$^{-/-}$*p53*$^{+/-}$ animals (<10%) also developed tumors with an onset similar to *tBrca1*$^{-/-}$*p53*$^{-/-}$ animals. Southern blot analysis of all *tBrca1*$^{-/-}$*p53*$^{+/-}$ thymic lymphomas examined shows loss of the remaining wild-type *p53* allele (Fig. 2B). A low incidence (<5%) of T-cell lymphomas was observed in *tBrca1*$^{-/-}$ mice in peripheral organs of older animals (~1-year-old). No difference in tumor incidence or onset was observed in *tBrca1*$^{-/-}$*bcl2* mice when compared with *bcl2* controls (data not shown). These findings suggest that p53 tumor suppressor function is stringently enforced in *tBrca1*$^{-/-}$ and *tBrca1*$^{-/-}$*bcl2* cells and that loss of p53 is required for thymic lymphoma development.

The accelerated onset and increased frequency of tumorigenesis observed in *tBrca1*$^{-/-}$*p53*$^{-/-}$ mice prompted the examination of telomere integrity and chromosomal structure in *tBrca1*$^{-/-}$*p53*$^{-/-}$ thymomas. FISH revealed loss of telomere sequence from chromosome ends of *tBrca1*$^{-/-}$*p53*$^{-/-}$ tumors (Fig. 2C, F and G). In addition, numerous chromosomal translocations were identified with fusions containing readily detectable interstitial telomeric DNA (Fig. 2F), as well as dicentric chromosomes and Robertsonian-like fusions with either trace amounts (Fig. 2D and E) or no detectable telomeric DNA at the fusion point. Analysis of chromosome structure by spectral karyotyping (SKY) (24) of thymic lymphoma cells from three different *tBrca1*$^{-/-}$*p53*$^{-/-}$ animals revealed the presence of clonal reciprocal and non-reciprocal chromosomal translocations (Fig. 2H–N and Table 3) that are not typically observed in *p53*$^{-/-}$ thymic lymphomas (22). SKY analysis of *tBrca1*$^{-/-}$*p53*$^{-/-}$ peripheral T-cells revealed the presence of only non-clonal chromosomal translocations, with an absence of any translocation events in *p53*$^{-/-}$ peripheral T-cells (Fig. 3).

DISCUSSION

Telomeres are chromosomal elements that serve a protective function in the maintenance of genome stability by suppressing erosion and/or ligation of chromosome ends (13). Chromosomes with defective telomere length and/or structure are more susceptible to forming end-to-end fusions that fail to segregate properly in mitosis, resulting in chromosomal breakage accumulation and DNA damage checkpoint activation. The addition of telomeric tracts by telomerase

Table 2. Increased aneuploidy and chromosomal abnormalities in *tBrca1*$^{-/-}$ peripheral T-cells

Genotype	Cells analyzed	Chromosomes per metaphase[a]	Aneuploid cells (%)	Total end-to-end fusions[b,c,d]	Fusions with telomeres[b]	Tri-radial-like structures[b]	Chromosome breaks[b]	Chromatid breaks[b]	Fragments[b,e]
p53$^{-/-}$	47	39.2 ± 2.7 (26–40)	8 (17.0)	3 (0.06/cell) 6.38%	2 (0.043/cell) 4.25%	0	1 (0.02/cell) 2.13 %	3 (0.06/cell) 4.26 %	7 (0.15/cell) 12.77 %
tBrca1$^{-/-}$*p53*$^{-/-}$	46	38.1 ± 6.7 (24–56)	28 (60.9)	40 (0.87/cell) 67.4%	19 (0.41/cell) 39.1%	26 (0.57/cell) 41.3 %	15 (0.33/cell) 21.7 %	20 (0.44/cell) 34.8 %	32 (0.70/cell) 45.7 %
Bcl2	51	39.6 ± 1.7 (30–40)	5 (9.8)	0	0	0	0	0	8 (0.16/cell) 15.7 %
tBrca1$^{-/-}$*Bcl2*	49	39.0 ± 3.6 (25–49)	15 (30.6)	15 (0.31/cell) 24.5%	9 (0.18/cell) 18.4%	13 (0.27/cell) 22.5 %	6 (0.12/cell) 12.2 %	16 (0.33/cell) 24.5 %	12 (0.24/cell) 24.5 %
Wild-type	46	40.0 ± 0.2 (39–40)	2 (4.3)	0	0	0	1 (0.02/cell) 2.2 %	0	3 (0.06/cell) 6.5%

Chromosome aberration classification was done as described earlier (58). Results shown are pooled from metaphase spreads from activated T-cell populations of three different animals per genotype.
[a]Chromosomes per metaphase presented as mean ± SD and range of chromosome numbers presented in parentheses.
[b]Numbers presented with incidence per cell are indicated in parentheses in the second row. In the third row, percentage of cells having aberrations are presented. Fusions with telomeres indicate that the chromosome fuses where telomeres are present at the fusion point.
[c]66.6% of *p53*$^{-/-}$ fusions, 47.5% of *tBrca1*$^{-/-}$*p53*$^{-/-}$ and 60% *of tBrca1*$^{-/-}$*bcl2* fusions have telomeres at the fusion point, respectively.
[d]Includes Robertsonian fusion-like configurations (p-arm fusions), telomere associations, dicentric chromosomes (q-arm fusions), ring-like structures (sister chromatid fusion) (58).
[e]Includes centric and acentric fragments.

compensates for the progressive loss of telomeric sequences from successive rounds of DNA replication.

Here, we provide evidence suggesting that Brca1 participates in the maintenance of telomere integrity. Furthermore, the observed telomere erosion phenotype in *tBrca1*$^{-/-}$ cells could conceivably precipitate genomic instability and p53 activation following *Brca1* disruption, which contribute to the observed defects in development, survival and proliferation (12). The mechanism whereby Brca1 loss precipitates telomere loss is not understood and appears to occur independent of factors that have been previously identified as regulators of telomere length and structure. The increased accumulation of chromosomal fragments detected in *tBrca1*$^{-/-}$*bcl2* and *tBrca1*$^{-/-}$*p53*$^{-/-}$ cells (Table 2) could be the result of catastrophic mitotic shearing in cells with fused chromosomes (19,22). Tri- and quadric-radial configurations in *tBrca1*$^{-/-}$*bcl2* and *tBrca1*$^{-/-}$*p53*$^{-/-}$ cells are a consequence of reciprocal exchange of double-stranded DNA, leading to chromatid exchange. The appearance of these structures has not been reported to occur as a consequence of telomere erosion and may reflect a telomere-independent mechanism of genomic instability, as Brca1 normally interacts with components of multiple DNA repair pathways (5,6,25). However, the formation of such structures has been observed to persist in telomerase-negative fibroblasts following exposure to γ-irradiation (26). Although our experimental approach does not distinguish the temporal relationship between loss of telomeres and onset of genome instability in Brca1-deficient cells, compelling evidence for telomere dysfunction contributing to genomic instability has been reported in yeast (27).

As Brca1 has been implicated in several apparently distinct processes that could impact genomic integrity, we are presently unable to dissect using our experimental approach which cellular process contributes to the Brca1 effect on telomere integrity. Several lines of evidence support a role for Brca1 in recombinational processes (5,25,28). The fact that Brca1 deficiency results in a generation-independent telomere shortening suggests that Brca1 could be involved in a telomerase-independent pathway of telomere maintenance that involves recombination (reviewed in 29,30). Components of the DNA damage response associated with DNA end-to-end joining or homologous recombination have been proposed to mediate alterations in telomere structure believed to be required for telomerase access (13–15). These activities have also been linked to 'telomere rapid deletion' in yeast, which has been proposed to reset telomere size during meiosis (31). Telomere rapid deletion has been defined as an end-mediated intrachromatid homologous-recombination event that results in a deleted telomere and a linear or circular by-product (31). Both Rad50 and Mre11 are required for telomere maintenance in yeast (32–36), and hypomorphic Rad50 mutant mice have been shown to exhibit attrition of telomere sequence in first-generation animals similar to Brca1-deficient cells (37). The components of the Mre11/Rad50/Nbs1 complex have been found to associate with the telomere binding proteins TRF1 and TRF2 (38,39). Previous studies have demonstrated interaction of human Mre11/Rad50/Nbs1 protein complex with Brca1 (40) consistent with a role in recombinational DNA repair (41,42). Further studies will be required to establish whether the attrition of telomere

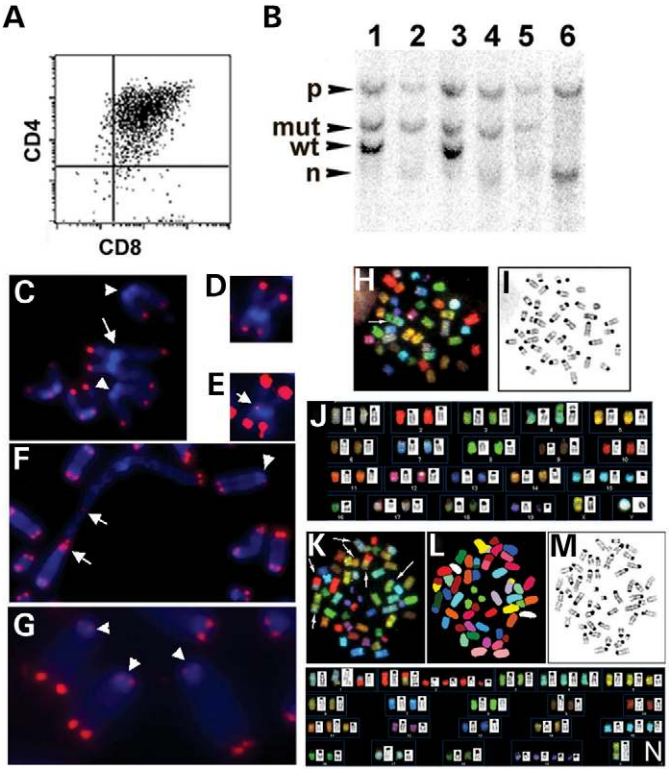

Figure 2. (**A**) Typical CD4 and CD8 profile of *tBrca1*$^{-/-}$*p53*$^{-/-}$ thymomas. (**B**) Representative Southern analysis of *p53* alleles in two *tBrca1*$^{-/-}$*p53*$^{+/-}$ mice (lane 1, tail; lane 2, thymoma for the first mouse; lane 3, tail; lane 4, thymoma for the second) compared with *tBrca1*$^{-/-}$*p53*$^{-/-}$ mouse (lane 5, tail; lane 6, thymoma) showing loss of wild-type (wt) and mutant (mt) alleles and generation of novel *p53* exon 4-containing hybridization fragment (*n*) in thymomas (lanes 2, 4 and 6). (**C**–**G**) Telomere-FISH analysis of *tBrca1*$^{-/-}$*p53*$^{-/-}$ tumors. Arrowheads denote chromosome ends with reduced telomere signal (C, F and G); arrows denote chromosomal fusions (C, E and F). Representative Robertsonian fusion-like chromosome (D and E) shown at normal exposure settings (D) and enhanced exposure to reveal telomeric signal at fusion point (E). Chromosomal fusion with interstitial telomeric signal (F). (C–E) Chromosomes from thymic lymphoma 2; (F–G) chromosomes from thymic lymphoma 3 (Table 3). (**H**–**N**) Structural and numerical chromosomal changes revealed by SKY analysis of *tBrca1*$^{-/-}$*p53*$^{-/-}$ tumors. (H–J) and (K–N) Representative metaphase cells from thymic lymphoma 2 and 3, respectively. (H and K) SKY RGB image visualizing each chromosome pair. Arrows indicate translocations observed as the juxtaposition of two colors within one chromosome. (I and M) Metaphase analysis using an inverted DAPI counterstain. (L) The same metaphase in (K) using pseudo-colors to aid identification. (J and N) Combined SKY and DAPI-banding karyotype analysis (Table 3).

Table 3. Karyotypes of *tBrca1*$^{-/-}$*p53*$^{-/-}$ thymomas by SKY analysis

Thymoma 1	Thymoma 2	Thymoma 3
[a]3 × 40, XX 7 × 34∼40, XX	10 × 40, XY	10 × 50, der(X)dup(X)(?E)t(X;17)(?F5;?B), −X/−Y
der(7)t(7;11)(F4;B4) [4] −13 [4] del(13)(C3) [2] der(19)t(14;19)(D3;D1)[2]	der(4;16)(A1;A1) [10] der(6)t(6;*)(F1;*) [3] +del(15)(A2::C) [10] del(19)(C1) [10]	t(1;3)(H1;H1) +der(1)t(1;2)(C3;F1) der(2)t(2;14)(C3;A2) +del(2)(C3)x4, + 4, +del(5)(G1) +der(11)t(11;?X)(B2;?) +15,del(17)(B::D) +del(19)(C2) × 2

Ten metaphases were analyzed per thymoma. Only clonal changes are shown and are described following ISCN 95 guidelines.
[a](), numbers indicate chromosomes participating on cytogenetic aberrations, letters followed by number identify particular chromosomal band involved; [], the total number of cells exhibiting a particular chromosomal change are shown. The karyotype for thymoma 3 was identical in all 10 metaphases analyzed. In different metaphases studied, three chromosomes (2, 13 and 14) underwent translocation to the band 6 (F1). der, derivative chromosome resulted from chromosomal change; del, deletion of specified chromosomal region; dup, duplication of specified chromosomal region; t, translocation.

sequences observed in our studies of Brca1-deficient T-cells is related to telomere maintenance associated with Mre11/Rad50/Nbs1 or other components of the DNA damage response pathway. Mammalian recombination-repair molecules DNA-PKcs (43–45), Ku (43,46–50) and PARP-1 (51) have been shown to be critical for maintenance of telomere integrity. Furthermore, recent studies of telomerase and the telomere proteins RIF1 and TRF2 have demonstrated broader roles in general DNA repair processes (52–54).

Telomere shortening in the absence of p53 has been previously shown to cooperate in tumorigenesis (17,22). The presence of clonal rearrangements in all tumors analyzed (Table 3) together with the presence of only non-clonal translocations in peripheral *tBrca1*$^{-/-}$*p53*$^{-/-}$ T-cells (Fig. 3) suggests that these rearrangements accelerate tumorigenesis observed in the thymus. Hence, loss of both Brca1 and p53 increases the propensity for formation of chromosomal translocations and thereby permits the fusion or deregulation of oncogenes at translocation breakpoints, together with deletions and unbalanced chromosomal translocations leading to loss of tumor suppressor genes. The observed heterogeneity of these clonal changes between tumors suggests that the synergistic effect of Brca1 and p53 on tumorigenesis can be achieved through multiple pathways that involve the generation of oncogenic translocations. The presence of such rearrangements is unusual in T-cells, in that reciprocal translocations are predominately associated (especially involving the antigen receptor loci) with lymphoid tumors, whereas non-reciprocal translocations are a characteristic feature of many solid tumors (55).

A substantial percentage of metaphases chromosomes in Brca1-deficient cells and tumors analyzed contained chromosomal translocations with telomeric DNA at the fusion site (Fig. 2 and Table 2). Telomere shortening has been shown to act synergistically with p53 deficiency in malignant transformation, presumably by enhancing genomic instability (17,22). Telomere erosion in telomerase-deficient mutant *p53* mice has been shown to contribute to tumorigenesis through generation of non-reciprocal translocations that likely occur through successive rounds of chromosomal fusion and breakage (22). Interestingly, breast tumors from these mice were also found to have non-reciprocal translocations, a cytogenetic feature of clinical breast cancer and other carcinomas (56). Hence, the presence of clonal chromosomal translocations containing telomeric DNA at the fusion points in *tBrca1*$^{-/-}$*p53*$^{-/-}$ thymomas is suggestive of the contribution of telomeric dysfunction. We propose that Brca1 deficiency results in two telomere-related outcomes: loss of telomere end maintenance (uncapping) and telomere

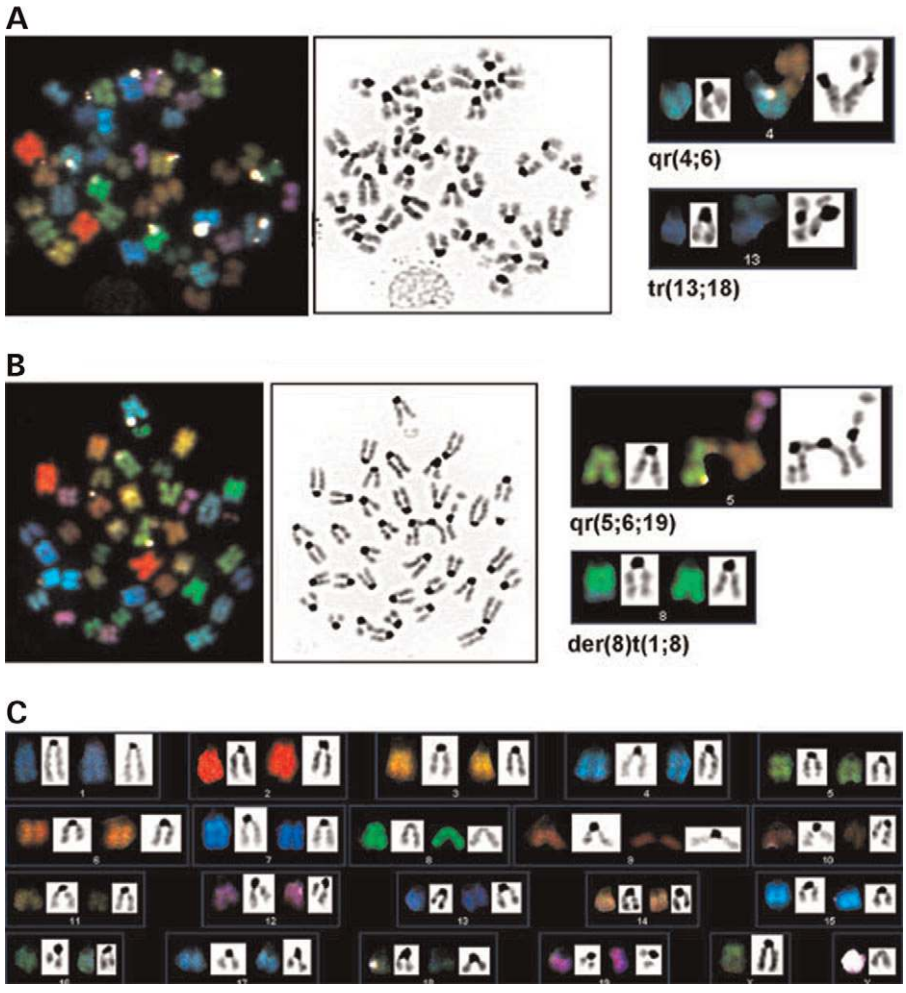

Figure 3. Structural and numerical chromosomal changes of $tBrca1^{-/-}p53^{-/-}$ (**A** and **B**) and $tBrca1^{+/-}p53^{-/-}$ peripheral T-cells (**C**) revealed by SKY analysis. (A) and (B) Representative analyses from two different metaphases (from left to right: SKY image, inverted DAPI counterstain, identification of chromosomal rearrangements) of T-cell population from the same $p53^{-/-}$ mouse that is homozygous for the *Brca1* mutation (contains the *Lck-cre* transgene and is homozygous for the conditionally disrupted Brca1 allele). In contrast to $tBrca1^{-/-}p53^{-/-}$ thymic lymphomas, all chromosomal translocations detected were non-clonal in nature. (C) Representative SKY karyotype analysis from T-cell population of $p53^{-/-}$ mouse that is heterozygous for the Brca1 mutation (contains the *Lck-cre* transgene and is heterozygous for the conditionally disrupted *Brca1* allele). No structural changes were detected.

length erosion. The observed synergy in tumorigenesis provides a rationale for the frequent mutation of p53 in human BRCA1 tumors (57). Our findings support a role for Brca1 in maintaining telomere stability and provide a rationale whereby disruption of BRCA1 in familial carriers contributes to tumorigenesis.

MATERIALS AND METHODS

Quantitative fluorescence *in situ* hybridization

$tBrca1^{-/-}$ mice ($Brca1^{fl5\text{-}6}$ mice bearing floxed *Brca1* alleles and the *Lck-Cre* transgene) crossed with $p53^{-/-}$ mice or *Eμ-bcl2-36* transgenic mice. Fluorescence-activated cell sorting analysis and preparation of anti-CD3ε activated peripheral T-cells have been previously described (12). FISH with Cy3-labeled $(CCCTAA)_3$ peptide nucleic acid and quantitative analysis of telomere fluorescence were performed as described previously (16). Telomere length measurements and chromosome karyotyping were performed blind from sibling pairs derived from three independent litters. To score the incidence of anaphase chromosome fusions, at least 100 anaphase events were scored from $p53^{-/-}$ and $tBrca1^{-/-}p53^{-/-}$ activated peripheral T-cells, following immobilization of cells on poly-L-lysine coated coverslips and DAPI staining. Data shown are the mean ± standard deviation from three independent experiments.

Native in-gel hybridization

Detection of telomeric 3′-overhangs was performed essentially as described (20). Native gels were hybridized with a $(TTAGGG)_4$ probe to ensure the absence of denatured DNA in sample lanes prior to hybridization with a $(CCCTAA)_4$ probe. To rule out non-specific degradation of double-stranded telomere sequence, gels were denatured and subsequently hybridized to $(CCCTAA)_4$.

Cytogenetic analysis/SKY

Cytogenetic preparations of thymoma samples (*tBrca1*$^{-/-}$*p53*$^{-/-}$) and peripheral T-cells (*tBrca1*$^{-/-}$*p53*$^{-/-}$ and *p53*$^{-/-}$) were made according to standard protocols (24). The SKY™ KIT probe cocktail from Applied Spectral Imaging (ASI, Carlsbad, CA, USA) was hybridized to all cytogenetic preparations. Metaphase images were captured using an SD 200 spectral bio-imaging system (ASI Ltd, MigdalHaemek, Israel) attached to a Zeiss microscope (Axioplan 2) using Spectral Imaging software (ASI). The images were analyzed using the SKYView software version 1.5 (ASI). For each sample, 10 SKY-metaphase spreads were karyotyped according to spectral and inverted DAPI images.

ACKNOWLEDGEMENTS

We thank L. Harrington, Y. Liu, A.S. Balajee, F. di Fagagna and A. Elia for advice and experimental assistance; S. Benchimol for critical reading of the manuscript; J. Marth and S. Cory for providing *Lck-Cre* and *Eμ-Bcl2-36* transgenic mice. This work was supported by grants from the Academic Research Fund, National University of Singapore and National Medical Research Council, Ministry of Health, Singapore (M.P.H.) and by grant #TFPP12000 from the National Cancer Institute of Canada and Amgen, Inc. (R.H.). J.P.M. was supported by a Medical Research Council of Canada fellowship.

Conflict of Interest statement. The authors have no conflicts of interest to declare.

REFERENCES

1. Welcsh, P.L., Owens, K.N. and King, M.C. (2000) Insights into the functions of BRCA1 and BRCA2. *Trends Genet.*, **16**, 69–74.
2. Starita, L.M. and Parvin, J.D. (2003) The multiple nuclear functions of BRCA1: transcription, ubiquitination and DNA repair. *Curr. Opin. Cell Biol.*, **15**, 345–350.
3. Shen, S.X., Weaver, Z., Xu, X., Li, C., Weinstein, M., Chen, L., Guan, X.Y., Ried, T. and Deng, C.X. (1998) A targeted disruption of the murine *Brca1* gene causes gamma-irradiation hypersensitivity and genetic instability. *Oncogene*, **17**, 3115–3124.
4. Xu, X., Weaver, Z., Linke, S.P., Li, C., Gotay, J., Wang, X.W., Harris, C.C., Ried, T. and Deng, C.X. (1999) Centrosome amplification and a defective G2-M cell cycle checkpoint induce genetic instability in BRCA1 exon 11 isoform-deficient cells. *Mol. Cell*, **3**, 389–395.
5. Moynahan, M.E., Chiu, J.W., Koller, B.H. and Jasin, M. (1999) Brca1 controls homology-directed DNA repair. *Mol. Cell*, **4**, 511–518.
6. Zhong, Q., Chen, C.F., Chen, P.L. and Lee, W.H. (2002) BRCA1 facilitates microhomology-mediated end joining of DNA double strand breaks. *J. Biol. Chem.*, **277**, 28641–28647.
7. Hartman, A.R. and Ford, J.M. (2002) BRCA1 induces DNA damage recognition factors and enhances nucleotide excision repair. *Nat. Genet.*, **32**, 180–184.
8. Gowen, L.C., Johnson, B.L., Latour, A.M., Sulik, K.K. and Koller, B.H. (1996) Brca1 deficiency results in early embryonic lethality characterized by neuroepithelial abnormalities. *Nat. Genet.*, **12**, 191–194.
9. Hakem, R., de la Pompa, J.L., Sirard, C., Mo, R., Woo, M., Hakem, A., Wakeham, A., Potter, J., Reitmair, A., Billia, F. *et al.* (1996) The tumor suppressor gene *Brca1* is required for embryonic cellular proliferation in the mouse. *Cell*, **85**, 1009–1023.
10. Liu, C.Y., Flesken-Nikitin, A., Li, S., Zeng, Y. and Lee, W.H. (1996) Inactivation of the mouse *Brca1* gene leads to failure in the morphogenesis of the egg cylinder in early postimplantation development. *Genes Dev.*, **10**, 1835–1843.
11. Ludwig, T., Chapman, D.L., Papaioannou, V.E. and Efstratiadis, A. (1997) Targeted mutations of breast cancer susceptibility gene homologs in mice: lethal phenotypes of Brca1, Brca2, Brca1/Brca2, Brca1/p53, and Brca2/p53 nullizygous embryos. *Genes Dev.*, **11**, 1226–1241.
12. Mak, T.W., Hakem, A., McPherson, J.P., Shehabeldin, A., Zablocki, E., Migon, E., Duncan, G.S., Bouchard, D., Wakeham, A., Cheung, A. *et al.* (2000) Brcal required for T cell lineage development but not TCR loci rearrangement. *Nat. Immunol.*, **1**, 77–82.
13. Blackburn, E.H. (2000) Telomere states and cell fates. *Nature*, **408**, 53–56.
14. Lansdorp, P.M. (2005) Major cutbacks at chromosome ends. *Trends Biochem. Sci.*, **30**, 388–395.
15. Viscardi, V., Clerici, M., Cartagena-Lirola, H. and Longhese, M.P. (2005) Telomeres and DNA damage checkpoints. *Biochimie*, **87**, 613–624.
16. Hande, M.P., Samper, E., Lansdorp, P. and Blasco, M.A. (1999) Telomere length dynamics and chromosomal instability in cells derived from telomerase null mice. *J. Cell Biol.*, **144**, 589–601.
17. Chin, L., Artandi, S.E., Shen, Q., Tam, A., Lee, S.L., Gottlieb, G.J., Greider, C.W. and DePinho, R.A. (1999) p53 deficiency rescues the adverse effects of telomere loss and cooperates with telomere dysfunction to accelerate carcinogenesis. *Cell*, **97**, 527–538.
18. van Steensel, B. and de Lange, T. (1997) Control of telomere length by the human telomeric protein TRF1. *Nature*, **385**, 740–743.
19. van Steensel, B., Smogorzewska, A. and de Lange, T. (1998) TRF2 protects human telomeres from end-to-end fusions. *Cell*, **92**, 401–413.
20. Hemann, M.T. and Greider, C.W. (1999) G-strand overhangs on telomeres in telomerase-deficient mouse cells. *Nucleic Acids Res.*, **27**, 3964–3969.
21. Zhang, X., Mar, V., Zhou, W., Harrington, L. and Robinson, M.O. (1999) Telomere shortening and apoptosis in telomerase-inhibited human tumor cells. *Genes Dev.*, **13**, 2388–2399.
22. Artandi, S.E., Chang, S., Lee, S.L., Alson, S., Gottlieb, G.J., Chin, L. and DePinho, R.A. (2000) Telomere dysfunction promotes non-reciprocal translocations and epithelial cancers in mice. *Nature*, **406**, 641–645.
23. McPherson, J.P., Lemmers, B., Hirao, A., Hakem, A., Abraham, J., Migon, E., Matysiak-Zablocki, E., Tamblyn, L., Sanchez-Sweatman, O., Khokha, R. *et al.* (2004) Collaboration of Brca1 and Chk2 in tumorigenesis. *Genes Dev.*, **18**, 1144–1153.
24. Liyanage, M., Coleman, A., du Manoir, S., Veldman, T., McCormack, S., Dickson, R.B., Barlow, C., Wynshaw-Boris, A., Janz, S., Wienberg, J. *et al.* (1996) Multicolour spectral karyotyping of mouse chromosomes. *Nat. Genet.*, **14**, 312–315.
25. Scully, R., Chen, J., Ochs, R.L., Keegan, K., Hoekstra, M., Feunteun, J. and Livingston, D.M. (1997) Dynamic changes of BRCA1 subnuclear location and phosphorylation state are initiated by DNA damage. *Cell*, **90**, 425–435.
26. Wong, K.K., Chang, S., Weiler, S.R., Ganesan, S., Chaudhuri, J., Zhu, C., Artandi, S.E., Rudolph, K.L., Gottlieb, G.J., Chin, L. *et al.* (2000) Telomere dysfunction impairs DNA repair and enhances sensitivity to ionizing radiation. *Nat. Genet.*, **26**, 85–88.
27. Hackett, J.A., Feldser, D.M. and Greider, C.W. (2001) Telomere dysfunction increases mutation rate and genomic instability. *Cell*, **106**, 275–286.
28. Scully, R., Chen, J., Plug, A., Xiao, Y., Weaver, D., Feunteun, J., Ashley, T. and Livingston, D.M. (1997) Association of BRCA1 with Rad51 in mitotic and meiotic cells. *Cell*, **88**, 265–275.
29. Dunham, M.A., Neumann, A.A., Fasching, C.L. and Reddel, R.R. (2000) Telomere maintenance by recombination in human cells. *Nat. Genet.*, **26**, 447–450.
30. Kass-Eisler, A. and Greider, C.W. (2000) Recombination in telomere-length maintenance. *Trends Biochem. Sci.*, **25**, 200–204.
31. Lustig, A.J. (2003) Clues to catastrophic telomere loss in mammals from yeast telomere rapid deletion. *Nat. Rev. Genet.*, **4**, 916–923.
32. Chamankhah, M. and Xiao, W. (1999) Formation of the yeast Mre11-Rad50-Xrs2 complex is correlated with DNA repair and telomere maintenance. *Nucleic Acids Res.*, **27**, 2072–2079.
33. Le, S., Moore, J.K., Haber, J.E. and Greider, C.W. (1999) RAD50 and RAD51 define two pathways that collaborate to maintain telomeres in the absence of telomerase. *Genetics*, **152**, 143–152.
34. Lundblad, V. (2002) Telomere maintenance without telomerase. *Oncogene*, **21**, 522–531.
35. Nugent, C.I., Bosco, G., Ross, L.O., Evans, S.K., Salinger, A.P., Moore, J.K., Haber, J.E. and Lundblad, V. (1998) Telomere maintenance

is dependent on activities required for end repair of double-strand breaks. *Curr. Biol.*, **8**, 657–660.
36. Usui, T., Ogawa, H. and Petrini, J.H. (2001) A DNA damage response pathway controlled by Tel1 and the Mre11 complex. *Mol. Cell*, **7**, 1255–1266.
37. Bender, C.F., Sikes, M.L., Sullivan, R., Huye, L.E., Le Beau, M.M., Roth, D.B., Mirzoeva, O.K., Oltz, E.M. and Petrini, J.H. (2002) Cancer predisposition and hematopoietic failure in Rad50(S/S) mice. *Genes Dev.*, **16**, 2237–2251.
38. Wu, G., Lee, W.H. and Chen, P.L. (2000) NBS1 and TRF1 colocalize at promyelocytic leukemia bodies during late S/G2 phases in immortalized telomerase-negative cells. Implication of NBS1 in alternative lengthening of telomeres. *J. Biol. Chem.*, **275**, 30618–30622.
39. Zhu, X.D., Kuster, B., Mann, M., Petrini, J.H. and de Lange, T. (2000) Cell-cycle-regulated association of RAD50/MRE11/NBS1 with TRF2 and human telomeres. *Nat. Genet.*, **25**, 347–352.
40. Zhong, Q., Chen, C.F., Li, S., Chen, Y., Wang, C.C., Xiao, J., Chen, P.L., Sharp, Z.D. and Lee, W.H. (1999) Association of BRCA1 with the hRad50-hMre11-p95 complex and the DNA damage response. *Science*, **285**, 747–750.
41. Lim, D.S., Kim, S.T., Xu, B., Maser, R.S., Lin, J., Petrini, J.H. and Kastan, M.B. (2000) ATM phosphorylates p95/nbs1 in an S-phase checkpoint pathway. *Nature*, **404**, 613–617.
42. Nelms, B.E., Maser, R.S., MacKay, J.F., Lagally, M.G. and Petrini, J.H. (1998) *In situ* visualization of DNA double-strand break repair in human fibroblasts. *Science*, **280**, 590–592.
43. Bailey, S.M., Meyne, J., Chen, D.J., Kurimasa, A., Li, G.C., Lehnert, B.E. and Goodwin, E.H. (1999) DNA double-strand break repair proteins are required to cap the ends of mammalian chromosomes. *Proc. Natl Acad. Sci. USA*, **96**, 14899–14904.
44. Gilley, D., Tanaka, H., Hande, M.P., Kurimasa, A., Li, G.C., Oshimura, M. and Chen, D.J. (2001) DNA-PKcs is critical for telomere capping. *Proc. Natl Acad. Sci. USA*, **98**, 15084–15088.
45. Hande, P., Slijepcevic, P., Silver, A., Bouffler, S., van, B.P., Bryant, P. and Lansdorp, P. (1999) Elongated telomeres in scid mice. *Genomics*, **56**, 221–223.
46. Bianchi, A. and de Lange, T. (1999) Ku binds telomeric DNA *in vitro*. *J. Biol. Chem.*, **274**, 21223–21227.
47. d'Adda di Fagagna, F., Hande, M.P., Tong, W.M., Roth, D., Lansdorp, P.M., Wang, Z.Q. and Jackson, S.P. (2001) Effects of DNA nonhomologous end-joining factors on telomere length and chromosomal stability in mammalian cells. *Curr. Biol.*, **11**, 1192–1196.
48. Hsu, H.L., Gilley, D., Blackburn, E.H. and Chen, D.J. (1999) Ku is associated with the telomere in mammals. *Proc. Natl Acad. Sci. USA*, **96**, 12454–12458.
49. Hsu, H.L., Gilley, D., Galande, S.A., Hande, M.P., Allen, B., Kim, S.H., Li, G.C., Campisi, J., Kohwi-Shigematsu, T. and Chen, D.J. (2000) Ku acts in a unique way at the mammalian telomere to prevent end joining. *Genes Dev.*, **14**, 2807–2812.
50. Samper, E., Goytisolo, F.A., Slijepcevic, P., van Buul, P.P. and Blasco, M.A. (2000) Mammalian Ku86 protein prevents telomeric fusions independently of the length of TTAGGG repeats and the G-strand overhang. *EMBO Rep.*, **1**, 244–252.
51. d'Adda di Fagagna, F., Hande, M.P., Tong, W.M., Lansdorp, P.M., Wang, Z.Q. and Jackson, S.P. (1999) Functions of poly(ADP-ribose) polymerase in controlling telomere length and chromosomal stability. *Nat. Genet.*, **23**, 76–80.
52. Bradshaw, P.S., Stavropoulos, D.J. and Meyn, M.S. (2005) Human telomeric protein TRF2 associates with genomic double-strand breaks as an early response to DNA damage. *Nat. Genet.*, **37**, 193–197.
53. Masutomi, K., Possemato, R., Wong, J.M., Currier, J.L., Tothova, Z., Manola, J.B., Ganesan, S., Lansdorp, P.M., Collins, K. and Hahn, W.C. (2005) The telomerase reverse transcriptase regulates chromatin state and DNA damage responses. *Proc. Natl Acad. Sci. USA*, **102**, 8222–8227.
54. Silverman, J., Takai, H., Buonomo, S.B., Eisenhaber, F. and de, L.T. (2004) Human Rif1, ortholog of a yeast telomeric protein, is regulated by ATM and 53BP1 and functions in the S-phase checkpoint. *Genes Dev.*, **18**, 2108–2119.
55. Atkin, N.B. (1986) Lack of reciprocal translocations in carcinomas. *Cancer Genet. Cytogenet.*, **21**, 275–278.
56. Heim, S. and Mittelman, F. (1995) *Cancer Cytogenetics*. Wiley-Liss, New York.
57. Crook, T., Crossland, S., Crompton, M.R., Osin, P. and Gusterson, B.A. (1997) p53 mutations in BRCA1-associated familial breast cancer. *Lancet*, **350**, 638–639.
58. Savage, J.R. (1976) Classification and relationships of induced chromosomal structural changes. *J. Med. Genet.*, **13**, 103–122.